Journal of Molecular Catalysis A: Chemical 385 (2014) 141–148

Contents lists available at ScienceDirect

Journal of Molecular Catalysis A: Chemical

journal homepage: www.elsevier.com/locate/molcata

Tuning of the catalytic properties of $PdCl_2(X_nPy)_2$ complexes by variation of the basicity of aromatic ligands

Agnieszka Krogul*, Jadwiga Skupińska, Grzegorz Litwinienko

Faculty of Chemistry, University of Warsaw, Pasteura 1, 02-093 Warsaw, Poland

ARTICLE INFO

Article history:
Received 13 November 2013
Received in revised form 22 January 2014
Accepted 26 January 2014
Available online 4 February 2014

Keywords:
Palladium complexes
Substituted pyridines
Thermal analysis
Crystal structure
Carbonylation

ABSTRACT

The position and number of substituents in pyridine ligands (X_nPy) were correlated with structural, physical, and chemical properties of $PdCl_2(X_nPy)_2$ complexes applied as catalysts for the carbonylation of aromatic nitrocompounds (phosgene-free method of carbamates production). Thermal stability and catalytic activity of $PdCl_2(X_nPy)_2$ complexes without steric hindrance increases with increasing X_nPy's basicity whereas a decrease of thermal stability and catalytic activity of the complexes is observed for sterically crowded complexes (with the *ortho*-substituted X_nPy). The complexes with X = Cl in *meta*- position of X_nPy decompose to a mixture of $PdCl_2$ and metallic Pd (similarly to complexes with Me_nPy) whereas complexes with *ortho*-chlorine (in X_nPy) decompose to the organopalladium products. Therefore, two different mechanisms of thermal decomposition are proposed for $PdCl_2(Cl_nPy)_2$ and $PdCl_2(Me_nPy)_2$. The results of complex thermal and structural analysis of a series of $PdCl_2(X_nPy)_2$ complexes allow us to get insight into the mechanism of nitrobenzene (NB) carbonylation catalyzed by $PdCl_2(X_nPy)_2$ at 150–180 °C. We conclude that ~~the~~ electron transfer from Pd(0) to nitrobenzene is the rate determining step of catalytic cycle of NB carbonylation.

1. Introduction

Polyurethanes belong to the most common polymers and their global production is still increasing, from 13.65 mln tonnes in 2010 to 17.95 mln tonnes expected by 2016 (with market value $55,480 mln) [1]. The polyurethanes are produced from methylene diphenyl diisocyanate (MDI) and toluene diisocyanate (TDI). Currently, the main method of industrial synthesis of isocyanates is a process employing phosgene – a toxic and relatively expensive gas produced from carbon monoxide and chlorine. The phosgene employing method is a potential source of species depleting the ozone layer and, therefore, needs to be eliminated [2]. The efforts to develop environmental friendly methods have been directed toward phosgene-free processes and one of the most promising method is the carbonylation of aromatic nitrocompounds catalyzed by transition metal complexes, leading to production of isocyanates and their precursors–carbamates (Scheme 1).

Although the yield and costs of catalytic carbonylation still cannot compete with the phosgene method, the carbonylation of nitro-compounds has additional advantage because it directly involves CO (without the step of phosgene synthesis from CO and Cl_2) giving an additional reduction of the costs [3–6].

There is a great interest in studies of more effective catalysts and Pd complexes receive much attention because of their relatively low cost (comparing to Rh and Ru compounds) and high effectiveness [7–15]. Recently, our research group have reported the system based on $PdCl_2(X_nPy)_2$ complexes (where: Py = pyridine, X = Me or Cl, $n = 0–2$) as the effective catalyst for carbonylation of nitrobenzene (NB) to ethyl *N*-phenylcarbamate (EPC) [16]. The current work aims to connect physical/chemical properties of $PdCl_2(X_nPy)_2$ with their catalytic activity and this is an extention of the research on Pd(II) complexes with substituted pyridines and their toxicity [17,18]. We also proposed the mechanism of carbonylation of NB with electron transfer from the palladium atom to nitrobenzene as the rate determining step as well as we determined spectral properties of $PdCl_2(X_nPy)_2$ in solution to confirm their square planar coordination geometry [16,17].

Carbonylation of NB to ethyl *N*-phenylcarbamate is carried out at relatively high-temperatures (150°–180 °C) and thermal stability of a catalyst is of crucial importance for its activity. Therefore, from the engineering point of view it is necessary to correlate the physical properties (particularly thermal stability) of Pd(II) complexes applied as catalysts with their catalytic activity in carbonylation. Thermal analysis (DSC and TG) seem to be the most appropriate for such studies of $PdCl_2(X_nPy)_2$.

---

* Corresponding author. Tel.: +48 22 8220211x378; fax: +48 22 8225996.
E-mail address: akrogul@chem.uw.edu.pl (A. Krogul).

1381-1169/$ – see front matter © 2014 Elsevier B.V. All rights reserved.
http://dx.doi.org/10.1016/j.molcata.2014.01.020

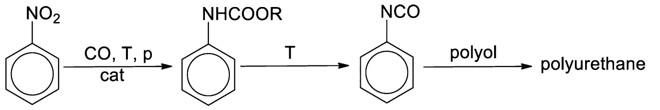

Scheme 1. Products of carbonylation of nitrobenzene in the presence of CO.

There are many examples of studies that deal with substituent effect in aromatic ring on properties of transtion metal (i.e. Fe, Cu) complexes with pyridine ligands [19]. Knowledge on the relationship between thermal stability of palladium(II) complexes and their catalytic activity will be also helpful in elucidation of mechanism of NB carbonylation in more details. Catalytic carbonylation can be described as a cyclic sequence of steps initiated by reaction of $PdCl_2(X_nPy)_2$ catalyst with aniline replacing the X_nPy ligands to form $PdCl_2(PhNH_2)_2$ that reacts with CO and X_nPy to give diphenylurea and $Pd^0(X_nPy)_2$ [16]. Subsequently, $Pd^0(X_nPy)_2$ complex reacts with nitrobenzene molecule and with CO. Rearrangements in cyclic intermediates lead to the formation of palladium–nitrene complex consecutively reacting with aniline. It is difficult to clearly distinguish whether the carbonylation occurs by a direct attack of aniline on the already coordinated molecule of CO or by a coordination of aniline to the metal, followed by attack of aniline on the adjacent coordinated CO. According to the literature both mechanisms are possible [4,20,21]. On the basis of calculation made by Hong et al. and on the basis of our own studies we suggest that both molecules, aniline and CO, are coordinated to Pd and then react [21]. After addition of another molecule of carbon monoxide, the complex decomposes with diphenylurea reacting immediately with ethanol to produce aniline and ethyl *N*-phenylcarbamate and the complex $Pd^0(X_nPy)_2$ is recovered and able to start next catalytic cycle [16]. All these processes form a catalytic cycle but at first, a replacement of X_nPy in $PdCl_2(X_nPy)_2$ complex by aniline initiates a series of carbonylations.

In this report we present thermal data for a series of $PdCl_2(X_nPy)_2$ complexes in order to correlate them with their catalytic activity. We hope the obtained data will be helpful during elucidation of detailed mechanism of the carbonylation process and during design and development of new Pd(II)-based catalysts.

2. Experimental

2.1. Materials

$PdCl_2$ was used as received. Pyridine (Py), substituted pyridines (2-MePy; 3-MePy; 4-MePy; 2,6-Me_2Py; 2,4-Me_2Py; 3,5-Me_2Py; 2-ClPy, 3-ClPy; 2,4-Cl_2Py), acetonitrile and acetone were distilled (or fractionally distilled) over the drying agent and stored under argon. Substituted pyridines: 2,6-Cl_2Py and 3,5-Cl_2Py were used as received.

2.2. Synthesis of $PdCl_2(X_nPy)_2$ (compounds **I–XII**)

The procedure has been described elsewhere [16]. Palladium chloride complexes with pyridines were prepared under argon. $PdCl_2$ (1.128 mmol) was placed in 10 mL flask equipped with magnetic stirrer and 2.26 mmol of Py or substituted X_nPy in 10 mL acetonitrile were added. Reaction was carried out at room temperature for 24 h. The elemental analyses of complexes **I**, **II**, **V**, **IX**, **XI** and **XII** were performed by a conventional method [16]. Single yellow crystals of **III**, **IV** and **VIII** obtained by a slow evaporation of their acetone solutions, were characterized by X-ray diffraction [17] and crystals of **VI**, **VII** and **X** are described in this work.

2.3. X-ray structure determinations

All measurements of crystal structure were performed on a KM4CCD κ-axis diffractometer with graphite-monochromated MoKα radiation. The crystals were positioned at 62 mm from the CCD camera. 1600 frames were measured at 0.5° intervals with a counting time of 11 s. The data were corrected for Lorentz and polarization effects. Empirical correction for absorption was applied [22]. Data reduction and analysis were carried out with the Oxford Diffraction programs [23]. The structures were solved by direct methods [24] and refined using SHELXL [25]. The refinement was based on F^2 for all reflections except those with very negative F^2. Weighted *R* factors *wR* and all goodness-of-fit *S* values are based on F^2. Conventional *R* factors are based on *F* with *F* set to zero for negative F^2. The $F_0^2 > 2\sigma(F_0^2)$ criterion was used only for calculating *R* factors and is not relevant to the choice of reflections for the refinement. The *R* factors based on F^2 are about twice as large as those based on *F*. All hydrogen atoms were located geometrically and their positions were refined. Temperature factors for some hydrogen atoms were fixed. Scattering factors were taken from Tables 6.1.1.4 and 4.2.4.2 [26]. The crystallographic data for the complexes are summarized in Table S1 (in Supplementary Material).

2.4. Thermal analysis, XRD and SEM measurements

Thermal stability of $PdCl_2(X_nPy)_2$ complexes was measured by Differential Scanning Calorimeter DSC 910 Du Pont Instruments (USA) connected to the thermal analyzer 9900 Computer/Thermal Analyzer and GBIP interface. The termogravimetric (TG) measurements were performed by means of termogravimeter Du Pont TGA 951 also connected to a thermal analyzer 9900 Computer/Thermal Analyzer and GBIP interface. All DSC and TG curves were recorded under nitrogen flow (6 dm^3/h), heating rate = 10 K/min. Thermal stability of the complexes was determined in temperature range 80–400 °C and mass of each sample was about 4 mg. Weight loss during thermal decomposition of $PdCl_2(X_nPy)_2$ was determined in temperature range 80–600 °C. TG measurements were performed in platinum cells and the average weight of sample was about 5–8 mg. Each result presented in this paper is the arithmetic mean of 3 repetitions and the difference of results in a series of determinations of the sample is up to 2%. Analysis of the products of thermal decomposition of $PdCl_2(X_nPy)_2$ complexes was carried out using powder diffractometer, working with copper lamp (radiation length 1.54) with a snap allowing to measure in the temperature range from 180 to 350 °C. The camera was equipped with a table for reflectometric measurements. Scanning electron microscope (SEM, model LEO 435 VP, Zeiss) equipped with an energy dispersive spectroscopy (EDS, Roentec) was used to examine the composition of the residue obtained after thermal decomposition of $PdCl_2(X_nPy)_2$ complexes.

2.5. Carbonylation procedure

The procedure has been described elsewhere [16]. Briefly, the reaction was carried out in a 200 mL stainless-steel autoclave equipped with magnetic stirrer. Before experiment, the autoclave was heated at 120 °C for 3 h and cooled down to room temperature. Subsequently, 0.056 mmol of catalyst $PdCl_2(X_nPy)_2$ and 2.68 mmol of Fe powder were placed in the autoclave, the air was evacuated and the system was filled with purified argon. Then, under an argon stream, other reagents and solvents were added: 0.12 mmol of I_2, 6.2 mmol of Py or X_nPy, 81 mmol of nitrobenzene or 27 mmol of nitrobenzene and 54 mmol of aniline; 20 ml ethanol (solvent). The amounts of nitrobenzene and aniline (27 and 54 mmol) are related to carbonylation of mixture of NB/AN in stoichiometric molar ratio

Table 1
Temperatures >of extrapolated start of decomposition T_{on} and temperatures of maximal heat release T_{max} for complexes **I–XII** together with their pK_a.

No.	$PdCl_2(X_nPy)_2$	Symbol	pK_a of X_nPy[a]	T_{on} (°C)	T_{max} (°C)
1	$PdCl_2(2,6\text{-}Me_2Py)_2$	**V**	6.20	254(292)[b]	291(300[b]
2	$PdCl_2(2,4\text{-}Me_2Py)_2$	**VI**	6.10	258	285
3	$PdCl_2(3,5\text{-}Me_2Py)_2$	**VII**	5.5	268	300
4	$PdCl_2(4\text{-}MePy)_2$	**IV**	5.43	252	283
5	$PdCl_2(2\text{-}MePy)_2$	**II**	5.38	224(260)[b]	247(278)[b]
6	$PdCl_2(3\text{-}MePy)_2$	**III**	5.17	226(248)[b]	235(266)[b]
7	$PdCl_2(Py)_2$	**I**	4.09	234	256
8	$PdCl_2(3\text{-}ClPy)_2$	**IX**	2.6	232	273
9	$PdCl_2(2\text{-}ClPy)_2$	**VIII**	2.0	184	207
10	$PdCl_2(3,5\text{-}Cl_2Py)_2$	**XII**	1.22	230	276
11	$PdCl_2(2,4\text{-}Cl_2Py)_2$	**XI**	1.4	181	206
12	$PdCl_2(2,6\text{-}Cl_2Py)_2$	**X**	0.97	128	162

[a] Basicity of X_nPy from Ref. [15].
[b] Two peaks are observed on DSC curves for complexes **V**, **II**, **III**.

1:2. The cover was closed and autoclave was directly filled with carbon monoxide (4 MPa), fixed, placed in a hot oil bath and kept at 180 °C for 1 or 2 h, depending on the reaction rate (see footnotes for Tables 2 and 3). After the reaction was completed, the autoclave was cooled in a water bath, then vented and a liquid sample of the reaction mixture was analyzed. The yield of the reaction was calculated on the basis of GC–FID and GC–MS analyses.

3. Results and discussion

Thermal stability was determined for twelve $PdCl_2(X_nPy)_2$ complexes (where: Py = pyridine; X = Me or Cl; n = 0–2) by means of differential scanning calorimetry (DSC) and thermogravimetry (TG). All DSC and TG curves were recorded under the same conditions (nitrogen atmosphere, heating rate = 10 K/min). The products of thermal degradation were analyzed by X-ray diffraction (XRD). Selected DSC and TG curves are shown in Fig. 1 (curves for other complexes are included in the Supplementary Material). Data obtained for all complexes are collected in Table 1 (DSC data) and Table 2 (TG).

Fig. 1 presents DSC and TG curves for $PdCl_2(3\text{-}MePy)_2$ (**III**) and $PdCl_2(3\text{-}ClPy)_2$ (**IX**). Comparing DSC and TG results it can be distinguished whether the effects observed on DSC curves correspond to a phase transition (mass = const.) or to the decomposition (heat ≠ const.; mass ≠ const.). The endothermic effects on DSC curves are observed as one peak as in Fig. 1A, or two, more or less separated peaks, as for complexes **II**, **III** and **V**, Fig. 1B. For **III** the first peak (in DSC curve) is not accompanied by the weight loss (in TG curve) indicating a phase transition (melting). Peaks for the complexes **II** and **V** overlap with temperature range of the weight loss (observed in TG curves), thus, the complexes **II** and **V** melt and decompose at the same time. Table 1 presents temperatures of the extrapolated start of decomposition T_{on} and temperatures of maximal heat release T_{max} for complexes **I–XII**.

The TG curves for $PdCl_2(X_nPy)_2$ complexes show one or two decomposition stages with the weight loss of 40.9–63.8%. Table 2 presents the data for complexes **I–XII** together with calculated mass losses and the assignments of degrading part of the complex for each decomposition step. The results depend on the nature of substituent(s) in the pyridine ring as well as on their positions. Observed differences might be a result of various mechanisms of decomposition of complexes with methyl- and chloropyridines.

TG curves indicate two-step decomposition of $PdCl_2(Me_nPy)_2$, except for complexes **VI** and **VII** (TG curves have no inflection, so they correspond to a single-step decomposition). For all $PdCl_2(Me_nPy)_2$ complexes the experimental weight loss is slightly larger than the expected for the elimination of two Me_nPy molecules and such data are in agreement with the results obtained by House [27], who suggested (on the basis of TG measurements, without chemical analysis of the residue) that decomposition of

Table 2
TG data: temperature range, experimental weight loss, calculated weight loss and assignments of eliminating part of $PdCl_2(X_nPy)_2$ for complexes **I–XII**[a].

No.	$PdCl_2(X_nPy)_2$	Symbol	Temperature range (°C)	Weight loss exp. (%)	Weight loss calc. (%)	Assignments
1	$PdCl_2(2,6\text{-}Me_2Py)_2$	**V**	263–330	26.0	27.4	$-Me_2Py$
			263–360	63.8	63.8	$-2Me_2Py$; -Cl
2	$PdCl_2(2,4\text{-}Me_2Py)_2$	**VI**	260–368	63.0	63.8	$–2Me_2Py$; -Cl
3	$PdCl_2(3,5\text{-}Me_2Py)_2$	**VII**	265–377	61.7	63.8	$-2Me_2Py$; -Cl
4	$PdCl_2(4\text{-}MePy)_2$	**IV**	258–352	51.5	51.2	-2MePy
			258–435	57.5	61.0	-2MePy; -Cl
5	$PdCl_2(2\text{-}MePy)_2$	**II**	238–318	49.6	51.2	-2MePy
			238–362	56.4	61.0	-2MePy; -Cl
6	$PdCl_2(3\text{-}MePy)_2$	**III**	238–336	41.0	25.6	-MePy
			238–481	51.3	51.2	-2MePy
7	$PdCl_2(Py)_2$	**I**	250–340	40.0	23.6	-Py
			250–465	50.5	47.2	-2Py; -Cl
8	$PdCl_2(3\text{-}ClPy)_2$	**IX**	256–363	59.4	56.2	-2ClPy
					64.9	-2ClPy; -Cl
9	$PdCl_2(2\text{-}ClPy)_2$	**VIII**	171–255	24.0	17.5	-2Cl
			171–320	40.9	45.6	-2Cl;-ClPy
10	$PdCl_2(3,5\text{-}Cl_2Py)_2$	**XII**	258–341	60.4	62.5	$-2Cl_2Py$
11	$PdCl_2(2,4\text{-}Cl_2Py)_2$	**XI**	188–261	27.0	15.0	-2Cl
			188–345	46.8	46.3	-2Cl; $-Cl_2Py$
12	$PdCl_2(2,6\text{-}Cl_2Py)_2$	**X**	131–204	21.5	15.0	-2Cl
			131–252	41.5	46.3	-2Cl; $-Cl_2Py$

[a] The products of thermal degradation were analyzed by X-ray diffraction (XRD). The presence of metallic palladium was detected in all complexes. For complexes **IX** and **XII** $PdCl_2$ were also detected in the residue.

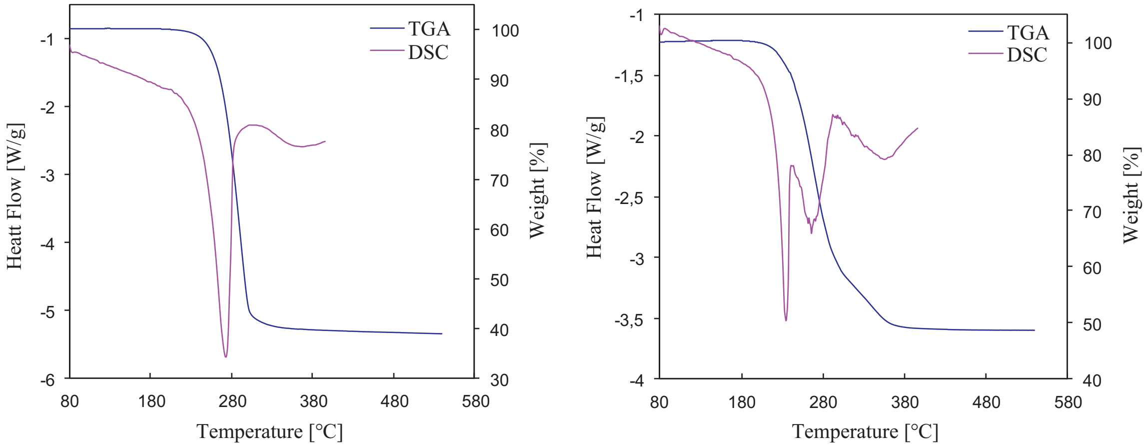

Fig. 1. DSC and TG curves for complexes: $PdCl_2(3\text{-}ClPy)_2$ (**IX**) and $PdCl_2(3\text{-}MePy)_2$ (**III**).

$PdCl_2(2,6\text{-}Me_2Py)_2$ and $PdCl_2(3,5\text{-}Me_2Py)_2$ gives a mixture of $PdCl_2$ and metallic Pd. Indeed, our XRD analysis of $PdCl_2(Me_nPy)_2$ decomposition products indicated the presence of metallic palladium, however, the residue was partially soluble in aqueous HCl giving a brown solution and it was a proof that other compounds apart from elemental Pd(0) were present in the products of thermal decomposition at 600 °C. Chlorine in the residue was detected by means of SEM measurements and we suggest that some polymeric structure of $PdCl_2$ was obtained, not identified by XRD as any known polymorph of $PdCl_2$. Summing up, our experiments with HCl, combined with the results of SEM and powder X-ray analysis are in agreement with the results described by other authors for decomposition of $PdCl_2$ complexes [28,29], therefore, we can state that the residue contains also palladium compounds other than Pd(0).

On the basis of literature data as well as the results obtained in this work we propose that thermal decomposition of $PdCl_2$ complexes with methylpyridines is at least two-step process with initial loss of two Me_nPy molecules followed by loss of chloride anion to form dimeric or polymeric palladium chloride. Decomposition of the complexes with $3\text{-}Cl_nPy$ proceeds in a similar way as the decomposition of $PdCl_2(Me_nPy)_2$ complexes: metallic palladium and $PdCl_2$ were found by XRD analysis of the residue and the polymorphic structure of residual $PdCl_2$ differs from a structure of $PdCl_2$ used in the synthesis. A different decomposition pattern can be observed for $PdCl_2(2\text{-}Cl_nPy)_2$ complexes (containing *ortho* substituted $2\text{-}Cl_nPy$ ligands). Data presented in Table 2 indicate that the first step corresponds to the elimination of two chlorine atoms followed by decomposition of one molecule of mono- or dichloropyridine ($2\text{-}Cl_nPy$), depending on the type of ligand. We suggest that during the first step a chlorine atom is removed from $PdCl_2$ and another Cl comes from $2\text{-}Cl_nPy$. Removal of two chlorine atoms from $PdCl_2$ is hardly possible, otherwise the same mechanism should take place for complexes with $3\text{-}Cl_nPy$, but the data listed in Table 2 show that the next step is the removal of a

Table 3
Selected bond distances (Å) and angles (°) for complexes **V–VII** and **X**[a].

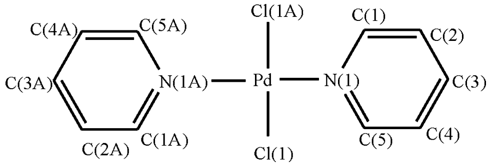

[a]

	***VI. VII. X** – this work*			**V** – literature data
Bond lenghts	**VI**	**VII**	**X**	**V**
Pd-N(1)	2.017(2)	2.0176(12)	2.0322(15)	2.0410(18)
Pd-N(1A)	2.017(2)	2.0176(12)	2.0322(15)	2.0410(18)
Pd-Cl(1)	2.2970(7)	2.3163(4)	2.3037(5)	2.3118(7)
Pd-Cl(1A)	2.2970(7)	2.3163(4)	2.3037(5)	2.3118(7)
N(1)-C(1)	1.329(3)	1.3456(19)	1.345(2)	1.355(3)
N(1)-C(5)	1.320(4)	1.3438(19)	1.341(2)	1.353(3)
N(1A)-C(1A)	1.329(3)	1.3456(19)	1.345(2)	1.355(3)
N(1A)-C(5A)	1.320(4)	1.3438(19)	1.341(2)	1.353(3)
Bond Angles				
N(1)-Pd-N(1A)	180.00	180.00	179.999(1)	180.00
N(1)-Pd-Cl(1)	89.69(5)	89.78(4)	89.78(4)	89.57(6)
N(1)-Pd-Cl(1A)	90.31(5)	90.22(4)	90.22(4)	90.43(6)
N(1A)-Pd-Cl(1)	90.31(5)	90.22(4)	90.22(4)	90.43(6)
N(1A)-Pd-Cl(1A)	89.69(5)	89.78(4)	89.78(4)	89.57(6)
Cl(1)-Pd-Cl(1A)	180.00	180.00	176.17(4)	179.9
C(1)-N(1)-Pd	118.9(2)	120.18(10)	121.45(13)	119.87(15)
C(5)-N(1)-Pd	122.8(2)	120.42(10)	121.90(13)	120.12(15)
C(1A)-N(1A)-Pd	118.9(2)	120.18(10)	121.45(13)	119.87(15)
C(5A)-N(1A)-Pd	122.8(2)	120.42(10)	121.90(13)	120.12(15)

[a] Schematic picture showing the order of the atoms.

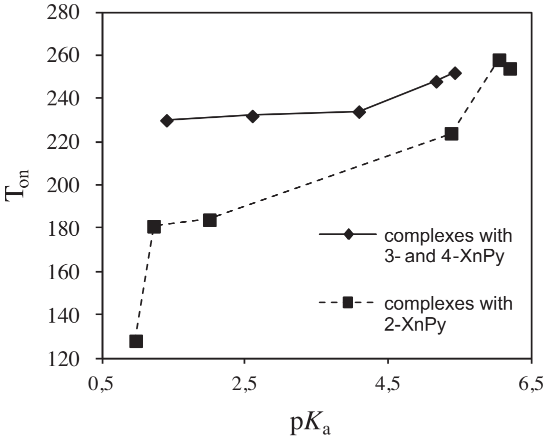

Fig. 2. Plots of temperatures of extrapolated start of thermal decomposition (T_{on}) of $PdCl_2(X_nPy)_2$ complexes versus pK_a values of X_nPy ligands with (■) and without (♦) *ortho* substituents.

whole 2-Cl_nPy ligand. Such sequence of decomposition indicates that there is still one molecule of organic ligand in the final product and we suggest the formation of organopalladium compound with C—Pd bond instead of C—Cl bond. Structures of mono- and dinuclear organopalladium compounds are described in the literature [30–34]. It can be concluded that position of substituent in the chloropyridine ring has a significant influence on the mechanism of the decomposition of $PdCl_2(Cl_nPy)_2$, a phenomena not observed for the complexes with methylpyridines.

As can be seen in Fig. 2 the increase of thermal stability (expressed as initial temperatures of decomposition, T_{on}) of complexes $PdCl_2(X_nPy)_2$ with the increase of pK_a of X_nPy ligands is observed. Significantly lower thermal stability of $PdCl_2(2\text{-}X_nPy)_2$ complexes is due to a steric hindrance in the complexes with *ortho*-substituted ligands. Such correlation between thermal stability of a complex and basicity of X_nPy ligand is accompanied by other relationships. The basicity of X_nPy ligand is strongly correlated with the catalytic activity of $PdCl_2(X_nPy)_2$ during nitrobenzene carbonylation to ethyl *N*-phenylcarbamate, see Fig. 3 where the activity of the complex is expressed as conversion of NB [16].

Taking into account the relationships between pK_a and thermal stability (Fig. 2) and between pK_a and conversion (Fig. 3) it can be easily predicted that thermal stability of the complex will be correlated with its activity. Indeed, Fig. 4 demonstrates that catalytic activity of $PdCl_2(X_nPy)_2$ complexes increases with increasing thermal stability. Concluding all three Figs. 2–4, the activity of $PdCl_2(X_nPy)_2$ depends on basicity and substitution pattern in X_nPy ligands, therefore, the strategies of design of new catalysts should be based on introduction of more electron-donating substituents into 3- or 4-position of pyridine ring.

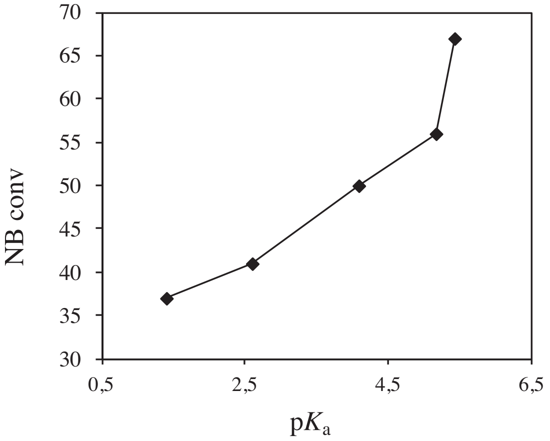

Fig. 3. Conversion of nitrobenzene (NB conv.) in the presence of $PdCl_2(X_nPy)_2$ versus pK_a of X_nPy for complexes without *ortho* substituted ligands. Conversion of nitrobenzene was determined for the following reaction conditions: $PdCl_2(X_nPy)_2$/Fe/I_2/X_nPy = 0.056/2.68/0.12/6.2 mmol; NB = 81 mmol; solvent (ethanol) = 20 ml; T = 180 °C; p(CO) = 4 MPa; time = 120 min. Py = pyridine (X = —CH_3, —Cl; n = 0–2).

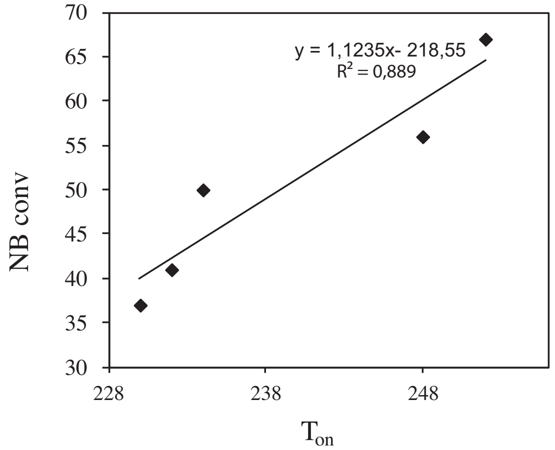

Fig. 4. Conversion of nitrobenzene (NB conv.) in the presence of $PdCl_2(X_nPy)_2$ versus temperatures >of extrapolated start of decomposition (T_{on}) of >$PdCl_2(X_nPy)_2$ complexes. >Conversion of nitrobenzene was determined for the reaction conditions described in the caption to Fig. 3. T_{on} was determined based on DSC measurements: under nitrogen flow (6 dm^3/h), in the temperature range 80–400 °C, heating rate = 10 K/min >and mass of each sample was about 4 mg.

We also investigated the substituent effects on the crystal structures of $PdCl_2(X_nPy)_2$ complexes in order to combine the results with thermal stability and catalytic activity. The crystallographic data for complexes of Pd(II) with Py and monosubstituted XPy (**I–IV**, **VIII** and **IX**) as well as for $PdCl_2(2,6\text{-}Me_2Py)_2$ are already known (structures of **III**, **IV** and **VIII** were characterized by our research group) [17,35–37], however, it was necessary to solve the crystal structures of complexes with disubstituted X_2Py (**VI**, **VII** and **X**) that have never been done before. We compared our results with available data for the whole series of complexes. Single yellow crystals of **VI**, **VII** and **X** were obtained by slow evaporation of the acetone solutions. All three crystalline compounds were found to be neutral mononuclear palladium complexes. The crystallographic data and details of structure refinements for these new complexes are presented in Supplementary Material, the selected bond distances (Å) and angles (°) collected for all complexes **V–VII** and **X** are collected in Table 3.

In complex **VI** (Fig. 5A) 2,4-dimethylpyridine rings show a *trans* disposition of methyl groups in *ortho* position and this phenomenon is the opposite to the disposition of *ortho* substituent in complexes with monosubstituted 2-XPy's (X = Me or Cl) [17]. The resulting crystals of $PdCl_2(2,4\text{-}Me_2Py)_2$ belong to monoclinic space group P 21/c. The angles formed between both 2,4-Me_2Py rings and the coordination plane are 85.05°. The square planar coordination geometry is confirmed by angles [N–Pd–Cl] = 89.69(5)° and 90.31(5)°. Crystals of complex **VII** belong also to monoclinic space group P 21/c, the crystallographic data for this complex are presented in Supplementary Material and its structure is shown in Fig. 5B. The ligand (3,5-dimethylpyridine) ring in **VII** is not orthogonal to the coordination plane and the dihedral angle between the coordination plane and the ligand ring plane is 57.05°. The square planar coordination geometry is confirmed by [N–Pd–Cl] angles, 89.78(4)° and 90.22(4)°, respectively (see Table 3). In contrast to **VI** and **VII**, the crystals of complex **X** belong to triclinic space group

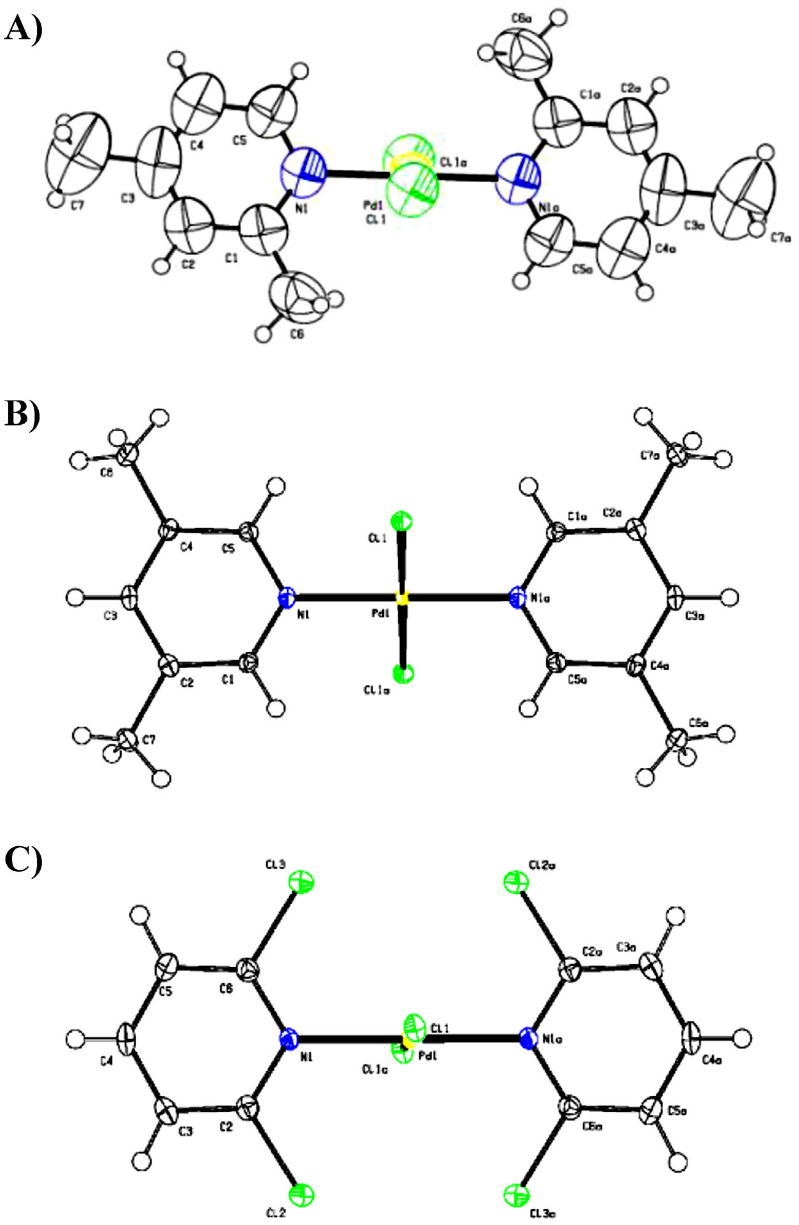

Fig. 5. SHELXL93 drawings of the molecular structures of: (A) $PdCl_2(2,4\text{-}Me_2Py)_2$ (complex **VI**), (B) $PdCl_2(3,5\text{-}Me_2Py)_2$ (complex **VII**), (C) $PdCl_2(2,6\text{-}Cl_2Py)_2$ (complex **X**). All drawings represent 50% probability.

P -1. As it was observed for **VI**, the aromatic rings in **X** are also orthogonal to the coordination plane and dihedral angle between coordination plane and ring plane is 86.14° and angles [N–Pd–Cl] are 90.22(4) and 89.78(4)°, respectively.

Our results obtained for **VI, VII** and **X** can be combined with the results for **I–V**, **VIII** and **IX** (accessible in database CSD: H. Allen, Acta Crystallogr., 2002, B58, 380) [17,33–35]. In the whole series of complexes the palladium ion coordinates two nitrogen atoms of pyridine ligands and two chlorine atoms in *trans* positions, exhibiting a square planar coordination geometry. We observe either *cis* or *trans* disposition of methyl/chlorine substituents in pyridine rings. For complexes with *ortho* monosubstituted XPy ligands the X is in *cis* disposition, whereas for sterically very similar disubstituted $2,4\text{-}Me_2Py$ ligands (complex **VI**) the *ortho* methyl groups are in *trans* position. *Trans* disposition of substituents is also observed in complexes with 3-MePy (complex **III**) and 3-ClPy (complex **IX**). Consequently, complexes **III**, **VI**, **IX** (with *trans* disposition of substituents in the X_nPy ring) as well as compounds with 4-Me (**IV**), $2,6\text{-}Me_2Py$ (complex **V**), $3,5\text{-}Me_2Py$ (complex **VII**), $2,6\text{-}Cl_2Py$ (complex **X**) and Py itself (**I**) have a centrosymmetric structure – a structural feature not observed for complexes with *ortho* monosubstituted ligands, i.e. 2-MePy (complex **II**) and 2-ClPy (complex **VIII**).

We did not find a direct correlation between ligand basicity and Pd—N bond length, similar in all investigated complexes (2.010–2.043 Å). The only observation is that Pd—N distances are slightly longer for complexes with Me_nPy comparing to complexes with Cl_nPy perhaps due to a greater contribution of back-donation of electrons from central atom into Cl_nPy than into Me_nPy, related to inductive effect of chlorine atoms [38]. A presence of *ortho* substituent in pyridine ring is manifested by increasing Pd–N distance in $PdCl_2(2\text{-}X_nPy)_2$. Except for this “effect of *ortho* group”, the introduction of *ortho*-methyl or *ortho*-chlorine in the pyridine ligand causes differences in the Pd—N—C bond angles. Another difference between the complexes with *ortho* substituted pyridines and the rest of complexes is that the ring plane is almost orthogonal to the coordination plane in $PdCl_2(2\text{-}X_nPy)_2$ – and this is observed for complexes with mono- and disubstituted ligands.

Because of low solubility of $PdCl_2(2,4\text{-}Cl_2Py)_2$ (**XI**) we did not determine the crystal structure of this compound. We have not found any literature data on *cis/trans* disposition of *ortho* chlorine atoms in the pyridine rings in **XI**. However, the comparative thermal analysis might be helpful method of indirect determination of structural features: the similar kinetic profiles of thermal decompositions of **XI** and $PdCl_2(2\text{-}ClPy)_2$ (complex **VIII**, with *cis* disposition, as well as complex **X**) support the hypothesis on the *cis* disposition of *ortho* substituents in **XI**.

The results of thermal analysis of $PdCl_2(X_nPy)_2$ complexes allow us to get insight into the mechanism of nitrobenzene (NB) carbonylation in the presence of $PdCl_2(X_nPy)_2$. Complexes with chloro- and dichloropyridines are thermally less stable than complexes with methyl- and dimethylpyridines. This observation is in agreement with our previous report that MePy's are better complexing agents than ClPy's [16]. Lability of a ligand has capital meaning because the initial step during nitrobenzene carbonylation requires a replacement of X_nPy ligands in $PdCl_2(X_nPy)_2$ complex by aniline. The Cl_nPy ligands can be replaced faster than Me_nPy ligands (better complexing agents). If this initial step limited the rate of carbonylation, the $PdCl_2(Cl_nPy)_2$ complexes would be more effective catalysts, however, complexes with Cl_nPy's are not better than the ones with Me_nPy's [16]. It means that a cleavage of Pd(II)—N(from X_nPy) bond is not the rate determining step (RDS) in the mechanism of carbonylation. Higher activity observed for more thermally stable complexes (with methylpyridines) might be caused by stronger pyridine coordination and these complexes remain catalytically active for a longer time. It also should not be excluded that lower catalytic activity of $PdCl_2(Cl_nPy)_2$ catalysts is caused by their lower thermal stability and different mechanism of thermal decomposition. In our previous paper we reported that another step, the electron transfer from Pd(0) to nitrobenzene is the RDS [16] and the complexation of X_nPy to Pd(0) seems to be more important for the reaction rate. In the present manuscript we exluded the pyridine substitution as the RDS, therefore, this observation is enforcing our previous hypothesis about nitrobenzene activation as RDS.

4. Conclusions

Results obtained from X-ray measurements indicate that nature and position of substituent in the aromatic ring is important to the structure of $PdCl_2(X_nPy)_2$ complexes. Pd—N bonds are slightly longer in complexes with $X = CH_3$ comparing to compounds with X = Cl. Introduction of X (=Cl, CH_3) in *ortho* position increases the Pd–N length and C–N–Pd angle values, however, we did not find a direct correlation between basicity of ligand and the Pd–N distance.

Taking into account data from thermal analysis and X-ray measurements, and combining them with the catalytic activity of $PdCl_2(X_nPy)_2$ complexes we found that for the complexes without steric hindrance (no *ortho*-substituted ligands) thermal stability and catalytic activity increase with increasing X_nPy's basicity. Presence of a substituent in the *ortho* position of the pyridine ring causes a decrease of thermal stability and catalytic activity of the complexes. Therefore, design of new catalysts should be based on introduction of more electron-donating substituents into 3- or 4-position of pyridine ring.

The effect of a substituent in the pyridine ring on the mechanism of thermal decomposition of $PdCl_2(X_nPy)_2$ complexes can be monitored by TG measurements. We propose different mechanism of $PdCl_2(Cl_nPy)_2$ decomposition comparing to $PdCl_2(Me_nPy)_2$ decomposition. Thermal stability and mechanism of degradation of $PdCl_2(Cl_nPy)_2$ complexes do not depend on the number of substituents in the pyridine ring but on their position in X_nPy: the complexes with chlorine in *meta*- position of Py decompose to mixture of $PdCl_2$ and metallic Pd (similarly to complexes with Me_nPy) whereas complexes with *ortho*-chlorine decompose to the organopalladium products. Thermal analysis can be helpful for indirect characterization of crystal structure of non-soluble $PdCl_2(X_nPy)_2$.

Finally, we can state that the replacement of X_nPy ligands in $PdCl_2(X_nPy)_2$ complex by aniline (the initial step of NB carbonylation process) is not a rate determining step. These results are consistent with the proposed elsewhere mechanism of catalytic carbonylation of nitrobenzene with the activation of nitrobenzene as the RDS.

Acknowledgement

This project was funded by the Ministry of Science and Higher Education (research project no. IP2011027071).

Appendix A. Supplementary data

Supplementary data associated with this article can be found, in the online version, at http://dx.doi.org/10.1016/j.molcata.2014.01.020.

References

[1] http://www.plastemart.com/Plastic-Technical-Article.asp?LiteratureID=674&Paper=global-polyurethane-market-PU-foams-thermoplastic-elastomers.
[2] T. Sakakura, J.-C. Choi, H. Yasuda, Chem. Rev. 107 (2007) 2365–2387.
[3] M. Tafesh, J. Weiguny, Chem. Rev. 96 (1996) 2035–2052.
[4] F. Ragaini, Dalton Trans. 32 (2009) 6251–6266.
[5] D.J. Diaz, A.K. Darko, L. McElwee-White, Eur. J. Org. Chem. 27 (2007) 4453–4465.
[6] J. Andraos, Pure Appl. Chem. 84 (2012) 827–860.
[7] F. Ragaini, S. Cenini, E. Gallo, A. Caselli, S. Fantauzzi, Curr. Org. Chem. 10 (2006) 1479–1510.
[8] F. Ragaini, S. Cenini, D. Brignoli, M. Gasperini, E. Gallo, J. Org. Chem. 68 (2003) 460–466.
[9] M. Gasperini, F. Ragaini, S. Cenini, E. Gallo, J. Mol. Catal. A 204 (2003) 107–114.
[10] T.L. Scott, B.C.G. Soderberg, Tetrahedron 59 (2003) 6323–6332.
[11] R. Santi, A.M. Romano, F. Panella, G. Mestroni, O. Santi, J. Mol. Catal. A: Chem. 144 (1999) 41–45.
[12] J. Skupińska, M. Karpińska, J. Mol. Catal. A 161 (2000) 69–73.
[13] J. Skupińska, M. Karpińska, Appl. Catal. 267 (2004) 59–66.
[14] J. Skupińska, M. Karpińska, M. Ołówek, Appl. Catal. 284 (2005) 147–154.
[15] J. Skupińska, M. Karpińska, M. Ołówek, T. Kasprzycka-Guttman, Cent. Eur. J. Chem. 3 (2005) 28–39.
[16] A. Krogul, J. Skupińska, G. Litwinienko, J. Mol. Catal: A. Chem. 337 (2011) 9–16.
[17] A. Krogul, J. Cedrowski, J. Wiktorska, W.P. Oziminski, J. Skupińska, G. Litwinienko, Dalton Trans. 41 (2012) 658–666.
[18] A. Krogul, J. Cedrowski, K. Wiktorska, W.P. Oziminski, J. Skupinska, G. Litwinienko, Bioorg. Med. Chem. Lett. 23 (2013) 2765–2768.
[19] P. Comba, M. Morgen, H. Wadepohl, Inorg. Chem. 52 (2013) 6481–6501.
[20] A.R.S. Mulla, C.V. Rode, A.A. Kelkar, S.P. Gupte, J. Mol. Catal. A: Chem. 122 (1997) 103–109.
[21] F.E. Hong, Y.C. Chang, Organometallics 23 (2004) 718–729.
[22] CrysAlis RED, Oxford Diffraction Ltd.,Version 1.171.28cycle2 beta (release 25-10-2005 CrysAlis171.NET) (compiled Oct 25 2005, 08:50:05). Empirical absorption correction using spherical harmonics, implemented in SCALE3 ABSPACK scaling algorithm.
[23] CrysAlis CCD, Oxford Diffraction Ltd., Version 1.171.28cycle2 beta CrysAlis RED, Oxford Diffraction Ltd.,Version 1.171.28cycle2 beta.
[24] G.M. Sheldrick, Acta Crystallogr. A46 (1990) 467–473.
[25] G.M. Sheldrick, SHELXL93, Program for the Refinement of Crystal Structures, University of Göttingen, Germany.
[26] A.J.C. Wilson (Ed.), International Tables for Crystallography. Volume C, Kluwer Academic Press, Dordrecht, 1992.
[27] R. Farran, J.E. House Jr., J. Inorg. Nucl. Chem. 34 (1972) 2219–2223.
[28] K.R. Chaudhari, A.P. Wadawale, V.K. Jain, J. Organomet. Chem. 698 (2012) 15–21.
[29] J. Perez, G. Sanchez, J. Garcia, J.L. Serrano, G. Lopez, J. Therm. Anal. Calorim. 66 (2001) 36–370.
[30] M.C. Navarro-Ranninger, M. Gayoso-Andrae, M.A. Alario-Franco, J. Therm. Anal. Calorim. 14 (1978) 281–290.

[31] V.A. Neto, A.E. Mauro, A.V.G. Netto, A.C. Moro, V.M. Nogueira, J. Therm. Anal. Calorim. 97 (2009) 57–60.
[32] N.D. Ball, J.W. Kampf, M.S. Sanford, Dalton Trans. 39 (2010) 632–640.
[33] A.C. Moro, A.E. Mauro, S.R. Ananias, A. Stevanato, A.O. Legendre, J. Therm. Anal. Calorim. 87 (2007) 721–724.
[34] J. Perez, G. Sanchez, J. Garcia, J.L. Serrano, G. Lopez, Thermochim. Acta 362 (2000) 59–70.
[35] P.B. Viossat, Acta Crystallogr. C 49 (1993) 84–85.
[36] M.C. Biagini, M. Ferrari, M. Lanfranchi, L. Marchiò, M.A. Pellinghelli, J. Chem. Soc., Dalton Trans. 10 (1999) 1575–1580.
[37] F. Zordan, L. Brammer, P. Sherwood, J. Am. Chem. Soc. 127 (2005) 5979–5989.
[38] D. Jaganyi, A. Hofmann, R. van Eldik, Angew. Chem. Int. Ed. 40 (2001) 1680–1683.